J Nanostruct 16(1): 585-594, Winter 2026

RESEARCH PAPER

Enhanced Properties of Composite Coatings by Nano Ceramic Powder on Titanium Alloy

Rusul S. Hadi *, Mohanad N. Al-Shroofy, Hanaa A. Al-Kaisy

Department of Materials Engineering, University of Technology, Baghdad, Iraq

ARTICLE INFO

Article History:
Received 11 September 2025
Accepted 19 December 2025
Published 01 January 2026

Keywords:
Bio-composite coating
Electrostatic spray method
Implants

ABSTRACT

The corrosion resistance of a titanium alloy (Ti6Al4V) can be improved while maintaining its mechanical properties by using an electrostatic spray technique. To develop the bio-composite polymer-based coating, various weight percentages (3, 6, 9, 12, and 15 wt.%) of Zirconium Oxide (ZrO_2) and Cerium Oxide (CeO_2) were blended with Polylactic Acid (PLA) powder in corresponding proportions (97, 94, 91, 88, and 85 wt.%), alongside a control coating of 100 wt.% PLA. The surface morphology of the coating layers was analyzed using FTIR and XRD. A contact angle test was conducted to calculate the biological behavior of the coated specimen, revealing favorable wetting properties. The resulting coatings exhibited high surface wettability and uniform, homogeneous, and crack-free layers.

How to cite this article
S. Hadi R., Al-Shroofy M., Al-Kaisy H. Enhanced Properties of Composite Coatings by Nano Ceramic Powder on Titanium Alloy. J Nanostruct, 2026; 16(1):585-594. DOI: 10.22052/JNS.2026.01.052

INTRODUCTION

The hard bone constitutes around 15% of total body weight and is recognized as the most extensive organ system in the human body. Basically, bone tissue is composed of a two-layered structure. The outer layer, referred to as cortical bone, accounts for roughly 80% of the overall bone mass in adults and exhibits low porosity of approximately 3–5% [1]. This layer provides strong torsional resistance in addition to bending, playing a significant role in structural integrity, weight-bearing capacity, and physical support. The internal layer, which consists of cancellous bone, produces a honeycomb-like network of trabeculae. It accounts for roughly 20% of total bone mass in adults and has a high porosity of 80–90% [2].

Acting as an inner support system, bone forms the human skeleton and is essential for maintaining motor functions, hematopoietic functions, in addition to protecting the nervous system and vital organs [3]. Roughly 70–80% of medical implants are produced by utilizing metallic biomaterials. These materials are frequently used in orthopedics for bone healing, fracture fixation, and load-bearing. Distinguished examples include 316L and 304L stainless steels, titanium, titanium-nickel alloys, tantalum, cobalt-based alloys (Co-Cr-Mo), and other metal-based materials [4, 5, 6]. To put it another way, metallic biomaterials remain a preferred choice for surgical implant production primarily because of properties that drove their primary acceptance years ago, including electrical conductivity, excellent formability, and strong fracture resistance [7]. Though challenges continue with these materials, especially their limited bioactivity, which hinders effective interaction with underlying cells. Surface modification methods have been improved to address these issues. These processes aim to roughen the material's surface to improve

* *Corresponding Author Email: Rusul.S.Hadi@uotechnology.edu.iq*

corrosion resistance, enhance biocompatibility, and facilitate integration with human bone and tissue. They also help increase fatigue resistance, decrease friction during motion, and improve surface hardness—factors that collectively extend the material's lifetime and overall performance. To this end, biopolymers, bioceramics, and carbon-based coatings are commonly applicable to metal implant surfaces to improve interface properties through refining surface morphology, roughness, hydrophilicity, and chemical characteristics [8, 9]. The current study has primarily focused on titanium alloys, with special attention to Ti-6Al-4V. This is chiefly because Titanium alloys have become the preferred material for the most advanced dental and medical applications today. Titanium alloy (Ti-6Al-4V) is principally known for its exceptional corrosion resistance, elevated biocompatibility and low toxicity, chemical stability, excellent mechanical properties, and moderately low Young's modulus, which has made it widely utilized in orthopedic surgery [10,11]. Upon exposure to air, a stable oxide layer forms on the surface of titanium alloys, providing bone-bonding properties when employed in implants. This notable corrosion resistance is attributed to the passive film that forms on the alloy's surface. For effective implant incorporation into bone tissue, the surface characterization of bone implants is critical. However, titanium and its alloys tend to have smooth surfaces, limited bioactivity, lower bone-bonding ability, and decreased wear resistance [12,13]. Several studies have shown that surface-altering techniques can reduce bacterial adhesion to implant surfaces, thereby potentially preventing biofilm formation and aiding bacterial clearance from the body. However, Ti6Al4V has low thermal conductivity (about 6.7 W/m · K), lower shear strength than steel and aluminum, and a high modulus of elasticity (about 114 GPa) [14]. These techniques improve the functionality of implanted biomaterials. Various coating methods are available, including chemical vapor deposition (CVD), plasma spraying, physical vapor deposition (PVD), micro-arc oxidation (MAO), sol-gel coating, electrophoretic deposition, and dip coating. All approaches have advantages and disadvantages that affect the resulting coating properties [15]. Dry coating technologies have been enhanced and adopted in both industrial and academic settings, highlighting efficiency and cost-effectiveness. These approaches offer different advantages compared to conventional powder deposition techniques, for example, decreased energy consumption, lower operational costs, and faster application times [16,17]. In electrostatic spray deposition, dry coating particles are fed into an electrostatic spray gun, where they are charged and evenly dispersed onto a prepared substrate without the need for water or solvents. Polymeric coatings have long been favored for protecting metals against corrosion because of their superior performance in harsh environments [18].

S.Cometa, M. Addolorata et al. (2019) In this study, Electrochemical deposition of polymers on metals has been recognized as a promising strategy for succeeding corrosion protection, benefiting from exact control utilizing microelectrodes. For example, paraffin wax and polylactic acid (PLA) were used as binders in a study that included stearic acid to enhance wettability and form strong bonds between the binder components [19]. In a 2021 study by Rasha A. Issa et al., a thin layer of polymethyl methacrylate (PMMA) containing embedded bio-ceramic particles (TiO_2 and Al_2O_3) was applied to 316L stainless steel by electrostatic deposition. The results showed a homogeneous, crack-free coating layer with unique mechanical properties [20]. More recently, in 2023, Samara Bashar et al. used the electrostatic spray technique to coat commercially pure titanium substrates with varying proportions of hydroxyapatite (HAP) mixed with PMMA and nickel oxide (NiO). Surface analysis performed utilizing XRD and FESEM/EDS showed homogeneous, uniform, and crack-free coatings along with improved surface wettability—a significant factor for biomedical implants [21]. Furthermore, M. Topuz et al. (2024). This research examined the synthesis, in vitro corrosion resistance, and adhesion performance of PLA-based composite coatings reinforced by halloysite nanotubes (HNT) and zirconia (ZrO_2) applied to beta-type Ti-30Zr-5Mo biomedical alloys. The sol-gel technique was used to prepare these coatings, which were subsequently characterized for surface morphology, chemical composition, and electrochemical properties. SEM analysis revealed cracks and micropores in specific coatings, while XPS and Raman spectroscopy confirmed the successful incorporation of HNT and ZrO_2 into the PLA matrix. Coatings containing HNT and ZrO_2, particularly in the HNT/ZrO_2 bilayer configuration, demonstrated a marked improvement in corrosion resistance. Additionally,

contact angle measurements confirmed the coatings' hydrophilic properties, essential for bioactive surfaces. This research underscores the potential of HNT and ZrO_2 reinforcements to enhance the bioactivity and corrosion resistance of Ti-30Zr-5Mo alloys, making them highly suitable for biomedical applications [22]. The electrostatic deposition technique to improve the surface of a titanium alloy (Ti6Al4V) substrate through making a biocomposite coating from a PLA-based composite with differing ratios of polylactic acid. The results proved that the coating layer adhered to the Ti6Al4V substrate in a homogeneous method, and the coated layers cut enhanced the biological activity and biocompatibility of the alloy.

In current work, Utilizing the ESD approach, PLA and ZrO_2/PLA, CeO_2/ PLA bio-composite coatings were employed to a Ti6Al4V substrate to enhanced their biocompatibility and the structural qualities of the coating.

MATERIALS AND METHOD

Alloy and metallographic preparations

Titanium alloy (Ti6Al4V) rod was sliced into samples by wire cut EDM with dimensions of (3 x 0.3cm) as a substrate, and they were utilized. The chemical composition of Ti6Al4V continuing, Fe (0.07) %, C (0.03) %, O (0.08) %, N(0.01)%, H(0.008)%. When cutting samples, wet-grinding with 100, 150, and 200 grit SiC sandpapers was used on the substrate surface to increase surface roughness. Following this, the samples were thoroughly cleaned to remove any residual rust and were rinsed sequentially with deionized water and alcohol. They were then completely dried and stored in a desiccator to maintain dryness before proceeding to the next step, which involved microstructure testing.

Composite Coating Preparations

Polymeric coating made of Polylactic acid (PLA) as a base composite material with several percentages of (3,9 &15) wt. % of ZrO_2 and CeO_2 bio-active ceramic particles as reinforcement material, blended in a ball mill for 30 min, prepared to use for uniform coating. The ZrO_2/PLA and CeO_2/PLA composite powders were prepared by mechanically combining ZrO_2 and CeO_2 powders with PLA in a mixing machine for 30 minutes. The mass ratios of ZrO_2 and CeO_2 to PLA for three types of ZrO_2/PLA, CeO_2/PLA composite powders were 3:97, 9:91, and 15:85.

Polylactic acid (PLA) as a base composite has a purity of about 99.8% with a particle size of 53 nm; zirconium dioxide has a purity of about 99.5% with a particle size of about 65 nm; and cerium oxide has a purity of about 99.9% with a particle size of <25 nm.

Generally, the ESD system consists of a stainless-steel capillary nozzle linked to a high-voltage power supply with positive polarity (COLO CL668W/30kV/PN) and a metallic substrate holder used for deposition. To control the thickness of the deposited layer, the voltage was set to 25 kV, and the distance between the substrate and the spray gun was maintained at 15 cm. The spraying process lasted 30 seconds. After deposition, the coated samples were heat-treated in an electric furnace at 160°C for 30 minutes.

RESULTS AND DISCUSSION

X- Ray Diffraction

The crystalline structure of the materials was examined utilizing an X-ray diffractometer (XRD Lab X-6000, SHIMADZU, Japan) featuring Cu radiation with a wavelength (1.54060 Å). Data collection was carried out across the 2θ range of 20° to 80°, utilizing a step size of 0.2° and a measurement duration of 1.20 seconds per step. The diffractometer was set to function at a voltage of 40 kV and a current of 30 mA. The resulting X-ray diffraction (XRD) pattern for the ZrO_2 layer exhibited crystalline structure with certain diffraction peaks is detected [23]. the major peaks (the most intense) correspond to ZrO_2: PLA in cubic phase five different diffraction peaks at 2θ values of 38.2°, 43.6°, 44.6°, 64.61°, and 77.54°, attributed crystal planes (111), (200), (220), (311), and (222) Consistent with the JCPDS card No. 03-065-0461 respectively. Similarly, all coated specimens with varying percentages of CeO_2: PLA displayed intense peaks at 2θ values of [24]. Also, some diffraction peaks corresponding to monoclinic phase are identified using the JCPDS card No. 00-037-1484; these peaks are attributed to planes (-111), (111), (200), (220), and (311) as represented in the XRD patterns of Fig. 1. The PLA resin materials exhibited broad highest peaks at 33.94° and 43.2° [25].

Representative of their amorphous nature, with extensive humps indicating the existence of a delicate PLA crystal lattice. The fusion of cerium oxide (CeO_2) and zirconium oxide (ZrO_2) in the polymer composite coating on Ti6Al4V resulted in

decreased peak intensities and slight shifts, likely due to the elevated tensile stress exerted through the substrate [26]. However, the reduction in peak height for the PLA-based composites might be due to X-ray absorption. The XRD patterns reveal the amorphous nature of the electrostatic coatings, as evidenced by the absence of crystalline peaks, indicating that the addition of $ZrO_2$and CeO_2 did not impact the structural properties of PLA. This result is due to the physical blending of ceramic

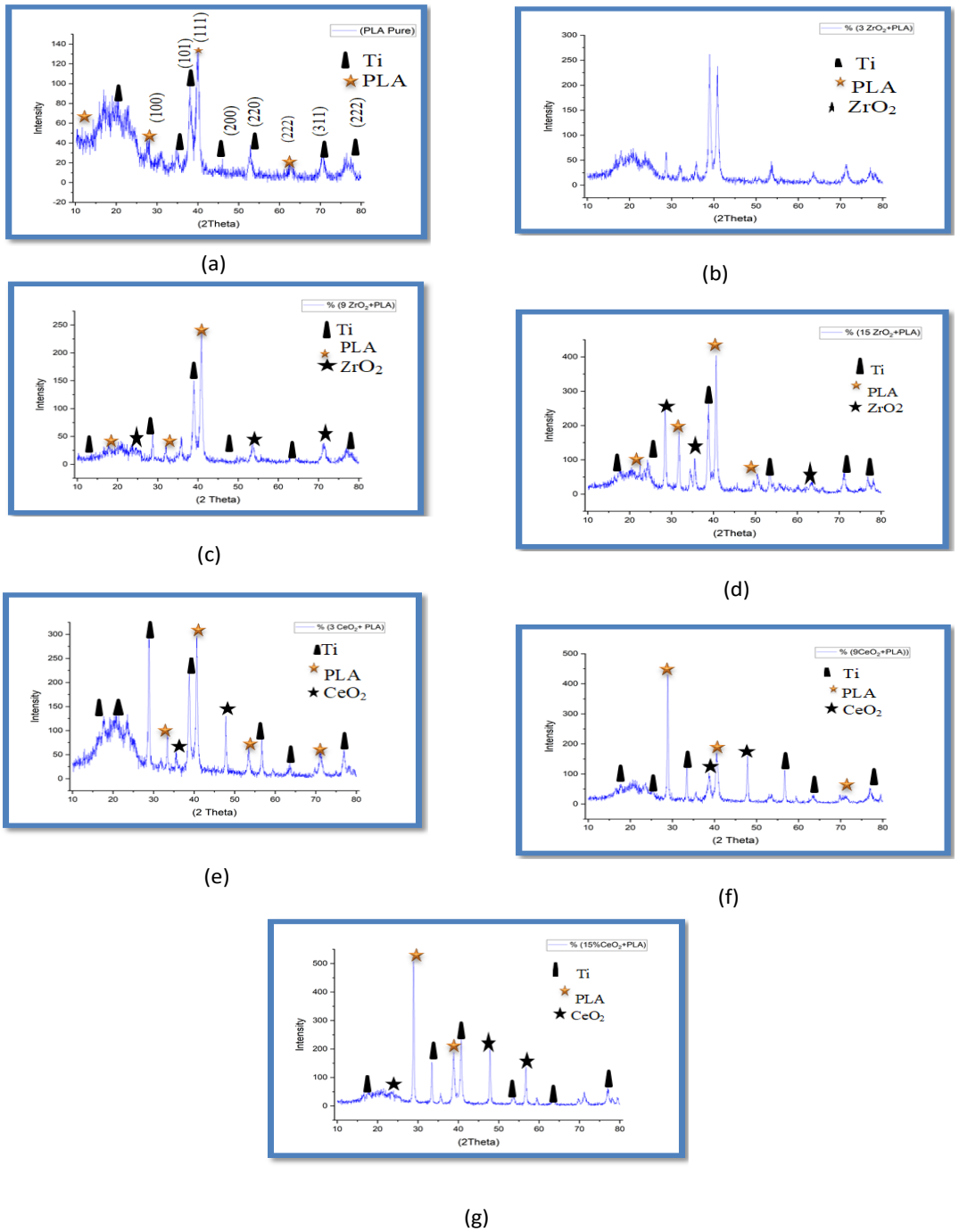

Fig. 1. X-ray diffraction (XRD) patterns of the coated specimens, (a)pure PLA, (b)PLA+3%ZrO_2, (C) PLA+9%ZrO_2, (d)PLA+15%ZrO_2, (e) PLA+3%CeO_2, (f) PLA+9CeO_2, (g) PLA+15%CeO_2.

particles with PLA, which occurs without triggering any chemical reactions.

FTIR Analysis

The FTIR spectrum presented in Fig. 2 confirms the successful deposition of the PLA coating as well as the PLA- ZrO_2/PLA- CeO_2 composite coating on the Ti6Al4V substrate. The FTIR spectrum of PLA shows absorbance at 2945.98 cm^{-1} and 2356.62 cm^{-1}, which correspond to the stretching

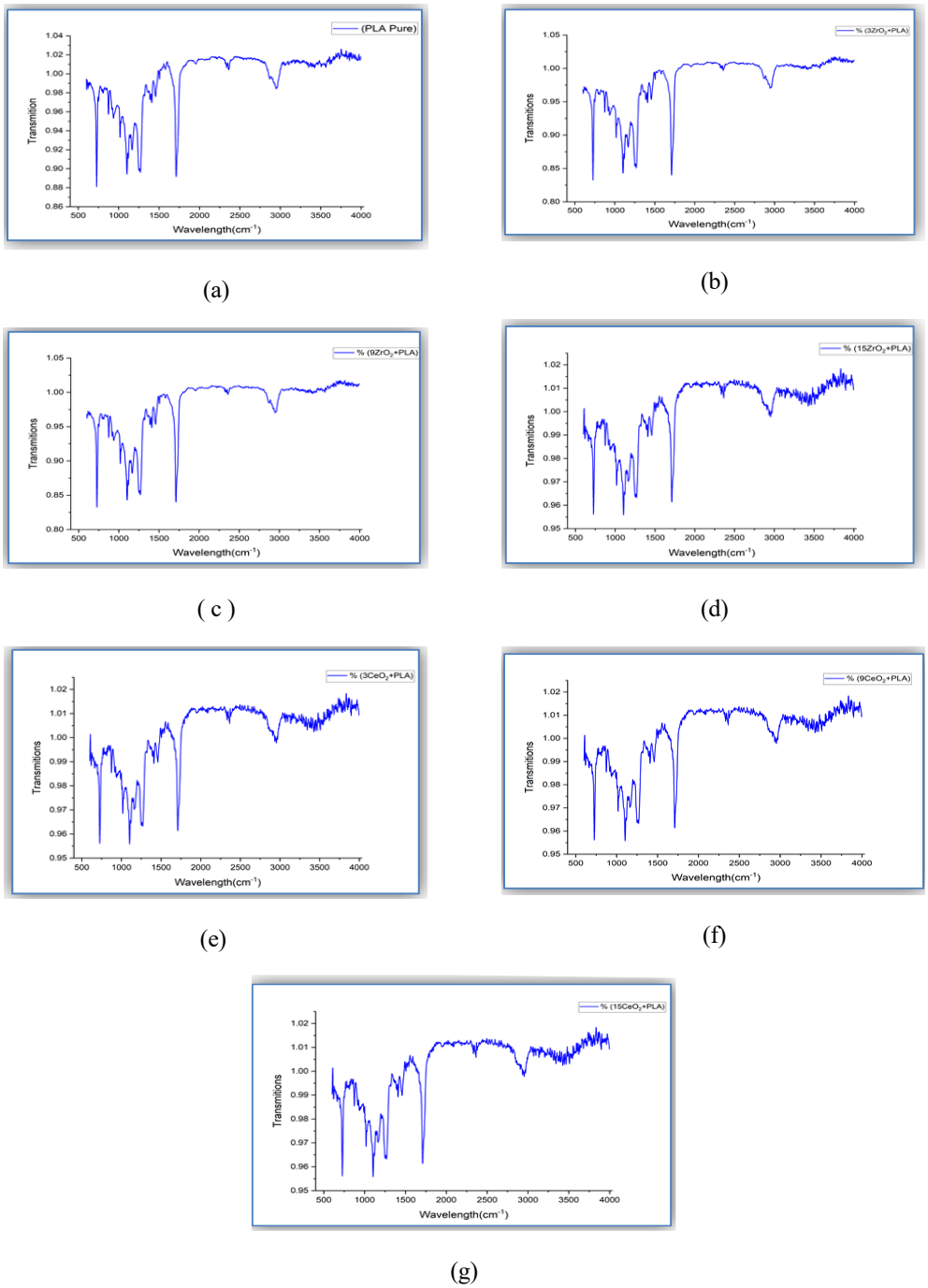

Fig. 2. FTIR of, (a)pure PLA, (b)PLA+3%ZrO_2, (C) PLA+9%ZrO_2, (d)PLA+15%ZrO_2,(e) PLA+3%CeO_2, (f) PLA+9CeO_2, (g) PLA+15%CeO_2.

vibrations of the C-H bonds within the alkane group. The peak at 1710.72 cm^{-1} is associated with C=O bending, while the absorbance at 1390.33 cm^{-1} relates to C-H vibrations. Additionally, sharp peaks at 1166.49 cm^{-1}, 1142.64 cm^{-1}, and 1017.54 cm^{-1} result from the stretching of C-O bonds in the ester group. Bending vibrations of C-H bonds are identified at 916.69 cm^{-1} and 873.85 cm^{-1}—distinct characteristics of the composite coatings, [27], including ZrO_2 and CeO_2, which are also evident in the spectra. A phosphate group stretching vibration is observed at 615.24 cm^{-1} [28,29].

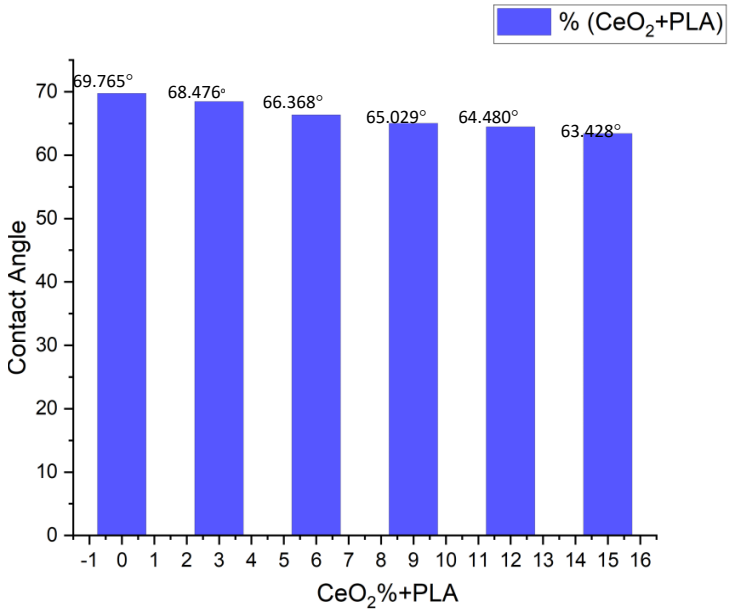

(a)

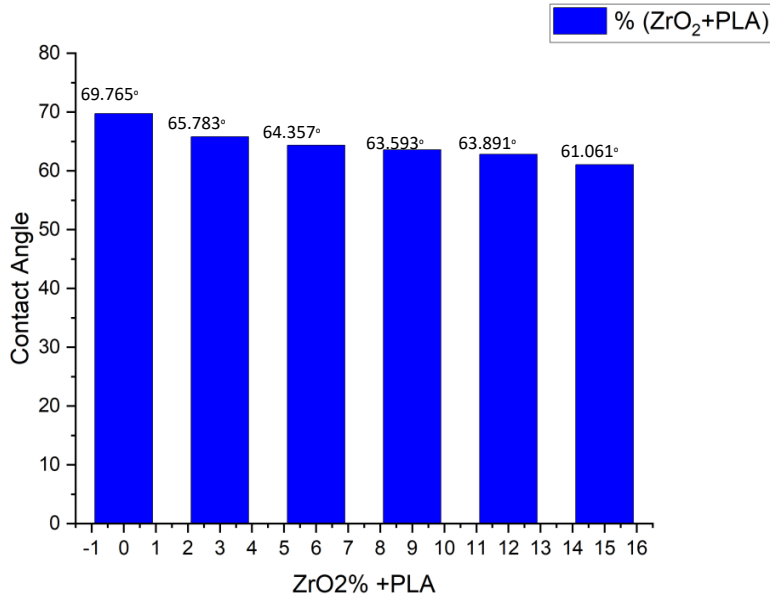

(b)

Fig. 3. Contact Angle of (a):(PLA+ CeO_2) wt.%, (b) :(PLA+ ZrO_2) wt.%.

The FTIR spectrum of the PLA- ZrO_2/PLA- CeO_2 composite reveals specific peaks corresponding to the individual features of PLA, ZrO_2, and CeO_2 materials. The noticed band shifts inside the coating indicate inter-component interactions. These results demonstrate that the PLA, CeO_2, and ZrO_2 components are efficiently integrated into the composite coating layer.

Contact Angle

The wettability assessment of a bioactive coated surface was taken by determining the contact angle formed by deionized water upon the test samples surface[30]. This examination proved the presence of a hydrophilic surface, recognized for its capability to attract and retain water, frequently shows a contact angle of under 90 degrees. Interestingly, some bacteria, for example S. aureus, are known to own hydrophobic properties. This feature contributes to their character as a chief pathogen in orthopedic infections and focuses the tendency of several bacteria to stick to hydrophobic surfaces. So, for bacterial adhesion to be decreased, important enhancements in the surface's hydrophilicity would be essential ,[31]. as exposed in Fig. 3a and b. The results presented that the primary contact angle of the coated surfaces was steadily under 90°. also, the water drops were noticed to be absorbed then diffused in the coating layer in

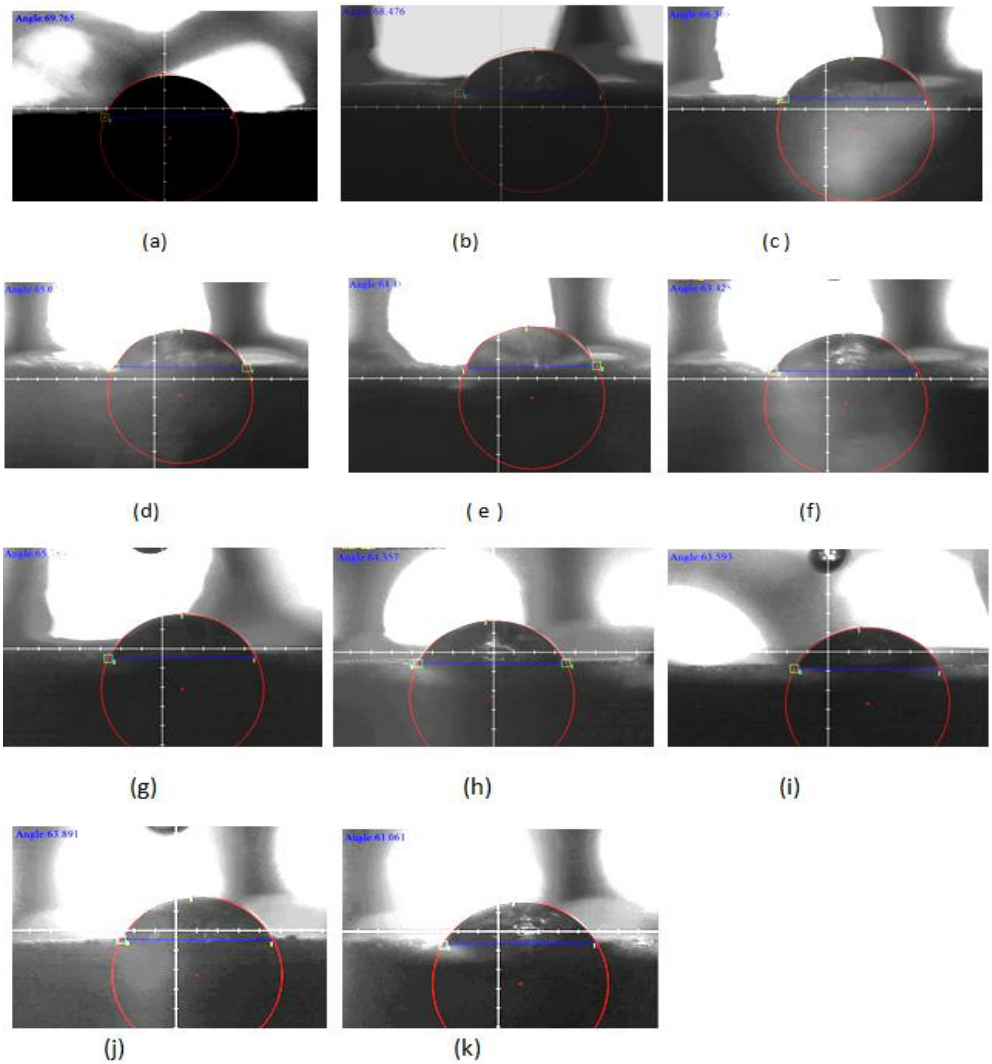

Fig. 4. samples of water droplet contact angles, (a)pure PLA,(b)PLA+3%ZrO_2, (c) PLA+6%ZrO_2, (d) PLA+9%ZrO_2, (e) PLA+12%ZrO_2, (f)PLA+15%ZrO_2, (g) PLA+3%CeO_2, (h) PLA+6%CeO_2, (i) PLA+9CeO_2, (j) PLA+12%CeO_2, (k) PLA+15%CeO_2.

wholly samples, representing good wettability. Especially, coatings incorporating CeO_2 (15wt.%) with percentage about (63.428) and ZrO_2 (15 wt.%) exhibited superior absorption with percentage (61.061) comparable to those prepared with pure PLA (69.756). An increase in CeO_2 and ZrO_2 particle content added reduced the contact angle, increasing absorption and promoting enhancing water drop dispersion.

Morphological Analysis (SEM)

The SEM/ EDS images of PLA, PLA/CeO_2, and PLA/ZrO_2 composite coatings, made with differing concentrations of PLA, ZrO_2, and CeO_2, correspondingly, by using an electrostatic potential of 25 kv for 30 seconds, are shown in Fig. 5. The PLA coating exhibited an ideal structure, a regular porous film, consistent with results from references [32] and [33], which discuss similar electrostatically deposited PLA coatings. All samples show that the implant surfaces were coated with smooth, crack-free layers that adhered successfully. The combined morphology of these coated films offers potential for improved antibacterial properties and corrosion resistance. The microscopic pores observed in the coatings,

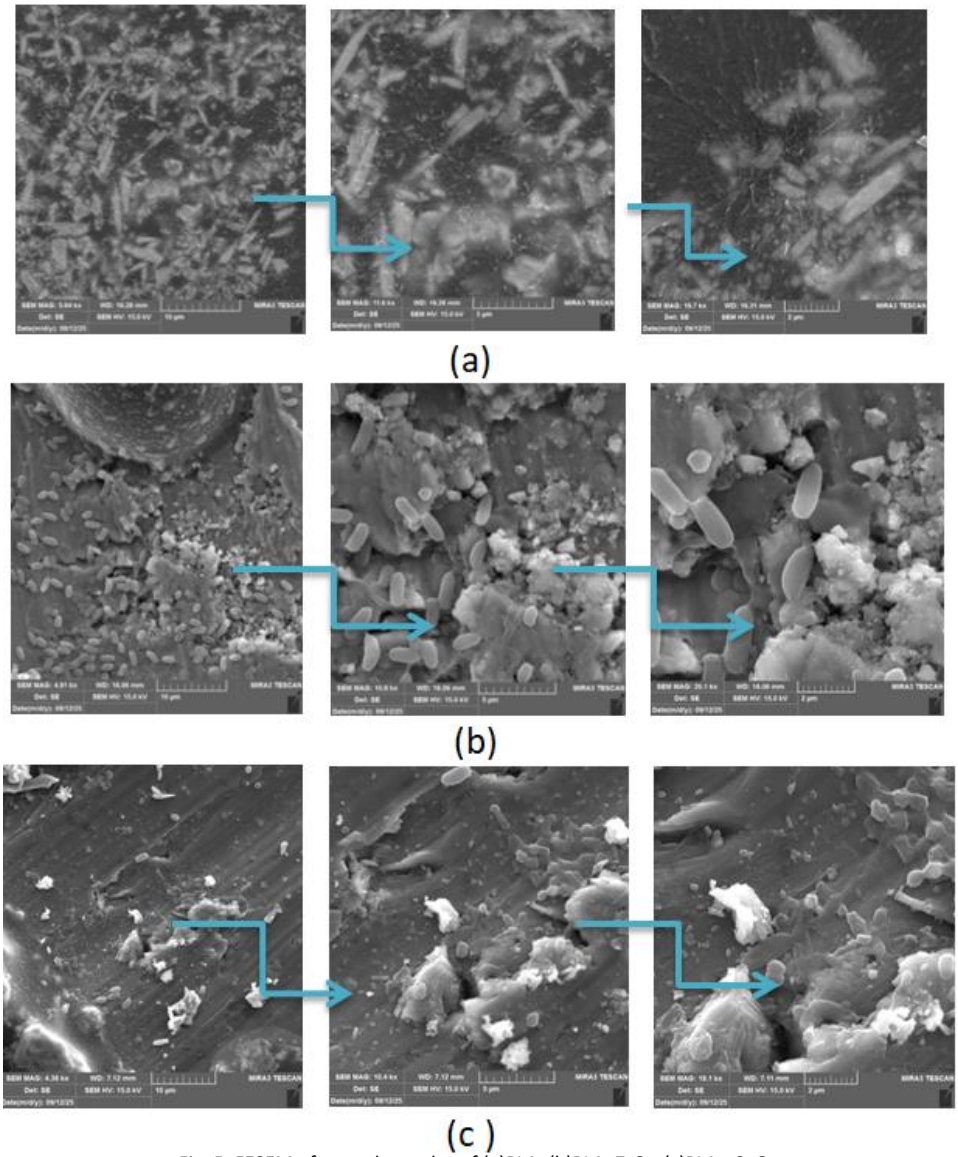

Fig. 5. FESEM of coated samples of (a)PLA, (b)PLA+ZrO_2, (c)PLA +CeO_2.

likely due to ZrO_2 and CeO_2 substitutions, suggest improved cell adhesion capabilities. The figure focuses on the homogeneous deposition of the coating layer and the uniform integration and distribution of ceramic particles in the PLA matrix. It exposes a balanced porosity amount with no significant cracks, offering good conditions for osseointegration. Notably, even though PLA particles partially melted during the heating method used to produce the film, they retained their spherical shape during deposition and curing.

CONCLUSION

Coated layers of ZrO_2/PLA and CeO_2/PLA composites were successfully applied through dry electrostatic deposition; XRD confirmed the presence of any chemical reaction among the composite components, and SEM micrographs showed coating morphological requisites, including homogenous distribution of reinforcing particles and uniform coating without cracks. Detecting the contact angle of the composite surface showed that the coating layers had significant wettability because of the hydrophilic nature of PLA combined with ZrO_2 particles, as well as CeO_2 particles, even though the wettability of ZrO_2 was greater than that of CeO_2. Coatings incorporating CeO_2 (15wt.%) with a percentage of about 63.428 and ZrO_2 (15 wt.%) exhibited superior absorption with a percentage of 61.061, comparable to those prepared with pure PLA (69.756). It is considered an important measure of how the human body works biologically and of its biocompatibility.

CONFLICT OF INTEREST

The authors declare that there is no conflict of interests regarding the publication of this manuscript.

REFERENCES

1. Han Y, You X, Xing W, Zhang Z, Zou W. Paracrine and endocrine actions of bone—the functions of secretory proteins from osteoblasts, osteocytes, and osteoclasts. Bone Research. 2018;6(1).
2. Parfitt AM. Misconceptions (2): turnover is always higher in cancellous than in cortical bone. Bone. 2002;30(6):807-809.
3. Clarke B. Normal Bone Anatomy and Physiology. Clin J Am Soc Nephrol. 2008;3(Supplement_3):S131-S139.
4. Harun WSW, Asri RIM, Alias J, Zulkifli FH, Kadirgama K, Ghani SAC, et al. A comprehensive review of hydroxyapatite-based coatings adhesion on metallic biomaterials. Ceram Int. 2018;44(2):1250-1268.
5. Sarker A, Tran N, Rifai A, Elambasseril J, Brandt M, Williams R, et al. Angle defines attachment: Switching the biological response to titanium interfaces by modifying the inclination angle during selective laser melting. Materials and Design. 2018;154:326-339.
6. Tran PA, Sarker A, Tran N, Jeffery C, Rifai A, Fox K. Coatings on metallic implants for biomedical applications. Metallic Biomaterials Processing and Medical Device Manufacturing: Elsevier; 2020. p. 359-385.
7. Biomedical Materials. Springer US; 2009. http://dx.doi.org/10.1007/978-0-387-84872-3
8. Sarker A, Tran N, Rifai A, Brandt M, Tran PA, Leary M, et al. Rational design of additively manufactured Ti6Al4V implants to control Staphylococcus aureus biofilm formation. Materialia. 2019;5:100250.
9. Saeed EM, Dawood NM, Hasan SF. Improvement corrosion resistance of Ni-Ti alloy by TiO_2 coating and hydroxyaptite/TiO_2 composite coating using micro arc oxidation process. Materials Today: Proceedings. 2021;42:2789-2796.
10. Abdel-Hady Gepreel M, Niinomi M. Biocompatibility of Ti-alloys for long-term implantation. J Mech Behav Biomed Mater. 2013;20:407-415.
11. Anjaneyulu U, Priyadarshini B, Arul Xavier Stango S, Chellappa M, Geetha M, Vijayalakshmi U. Preparation and characterisation of sol–gel-derived hydroxyapatite nanoparticles and its coatings on medical grade Ti-6Al-4V alloy for biomedical applications. Materials Technology. 2017;32(13):800-814.
12. Karthik D, Arul Xavier Stango S, Vijayalakshmi U, Swaroop S. Electrochemical behavior of laser shock peened Inconel 625 superalloy. Surf Coat Technol. 2017;311:46-54.
13. Kamachimudali U, Sridhar TM, Raj B. Corrosion of bio implants. Sadhana. 2003;28(3-4):601-637.
14. Wei G, Tan M, Attarilar S, Li J, Uglov VV, Wang B, et al. An overview of surface modification, A way toward fabrication of nascent biomedical Ti–6Al–4V alloys. Journal of Materials Research and Technology. 2023;24:5896-5921.
15. Xue T, Attarilar S, Liu S, Liu J, Song X, Li L, et al. Surface Modification Techniques of Titanium and its Alloys to Functionally Optimize Their Biomedical Properties: Thematic Review. Frontiers in Bioengineering and Biotechnology. 2020;8.
16. Valerolactone: An Alternative Solvent for Manufacturing of Lithium-Ion Battery Electrodes. American Chemical Society (ACS).
17. Al-Shroofy M, Zhang Q, Xu J, Chen T, Kaur AP, Cheng Y-T. Solvent-free dry powder coating process for low-cost manufacturing of LiNi1/3Mn1/3Co1/3O2 cathodes in lithium-ion batteries. J Power Sources. 2017;352:187-193.
18. Zhang Y, Liu J, Xu W, Lu Y, Ma H, Cheng F, et al. Gradient doping Mg and Al to stabilize Ni-rich cathode materials for rechargeable lithium-ion batteries. J Power Sources. 2022;535:231445.
19. Cometa S, Bonifacio MA, Mattioli-Belmonte M, Sabbatini L, De Giglio E. Electrochemical Strategies for Titanium Implant Polymeric Coatings: The Why and How. Coatings. 2019;9(4):268.
20. Prasad LK, McGinity JW, Williams RO. Electrostatic powder coating: Principles and pharmaceutical applications. Int J Pharm. 2016;505(1-2):289-302.
21. Al-Rashidy ZM, Farag MM, Abdel Ghany NA, Ibrahim AM, Abdel-Fattah WI. Orthopaedic bioactive glass/chitosan composites coated 316L stainless steel by green electrophoretic co-deposition. Surf Coat Technol. 2018;334:479-490.
22. Maleki-Ghaleh H, Khalil-Allafi J. Effect of hydroxyapatite-

titanium-MWCNTs composite coating fabricated by electrophoretic deposition on corrosion and cellular behavior of NiTi alloy. Mater Corros. 2019;70(11):2128-2138.
23. Yin D, Pan Y, Wang Y, Guo Q, Hu S, Huang J. Preparation and performance of electroless silver composite films based on micro-/nano-cellulose. Wood Science and Technology. 2022;56(2):649-668.
24. Chavarría-Bolaños D, Vega-Baudrit J, Cerda-Cristerna BI, Pozos-Guillén A, Montero-Aguilar M. Translation of Tissue Engineering Approach from to Clinics. Current Advances in Oral and Craniofacial Tissue Engineering: CRC Press; 2020. p. 24-35.
25. Sasmita M, Nathsarma SK, Mishra KG, Paramguru RK. Antimicrobial Activity of Silver Nanoparticles on Pseudomonas aeruginosa: Influence of Particle Size Controlled through Mixed Current. Surface Engineering and Applied Electrochemistry. 2022;58(2):184-193.
26. Falodun OE, Oke SR, Olubambi PA. Synthesis and Characterization of Commercial Pure Titanium-nickel Alloy Behavior Reinforced With Titanium Diboride. Research Square Platform LLC; 2020.
27. Liu-Snyder P, Webster TJ. Developing a New Generation of Bone Cements With Nanotechnology. Current Nanoscience. 2008;4(1):111-118.
28. Ismail N, Mohamad H, Ahmad N. Fabrication and characterization of 45S5 bioactive glass microspheres. AIP Conference Proceedings: AIP Publishing; 2020.
29. Rouein Z, Jafari H, Pishbin F, Mohammadi R, Simchi A. Biodegradation behavior of polymethyl methacrylate–bioactive glass 45S5 composite coated magnesium in simulated body fluid. Transactions of Nonferrous Metals Society of China. 2022;32(7):2216-2228.
30. Maleki-Ghaleh H, Khalil-Allafi J. Characterization, mechanical and in vitro biological behavior of hydroxyapatite-titanium-carbon nanotube composite coatings deposited on NiTi alloy by electrophoretic deposition. Surf Coat Technol. 2019;363:179-190.
31. Quinn J, McFadden R, Chan C-W, Carson L. Titanium for Orthopedic Applications: An Overview of Surface Modification to Improve Biocompatibility and Prevent Bacterial Biofilm Formation. iScience. 2020;23(11):101745.
32. Bashar S, Al-Kaisy HA, Al-Shroofy MN. Enhance the biocompatibility of titanium substrate by applying PMMA/Nb_2O_5 composite coating using electrostatic deposition. AIP Conference Proceedings: AIP Publishing; 2024. p. 080029.
33. Bashar S, Al-Kaisy HA, Al-Shroofy MN. Characterization of the wettability of bio-composite coating on titanium alloy using electrostatic spray deposition. AIP Conference Proceedings: AIP Publishing; 2023. p. 030037.